WFC3 Instrument Science Report 2008-37

WFC3 TV3 Testing: UVIS Science Monitor

H. Bushouse
November 25, 2008

ABSTRACT

Ten runs of the UVIS science monitor program were executed during WFC3 Thermal-Vacuum test #3, which provides a performance monitor of the UVIS channel via bias, dark, flat field, PSF, and throughput test exposures. The results show very good repeatability and stability of all measured performance parameters and that the UVIS channel easily meets or exceeds nearly all of the Contract End Item requirements that can be assessed with these data.

Introduction

During Wide Field Camera 3 (WFC3) system-level thermal-vacuum testing campaign #3 (TV3), which took place at Goddard Space Flight Center from February to April 2008, the UVIS Science Monitor test was executed periodically in order to assess and monitor the overall performance of the camera over the 2-month duration of TV3. The science monitor includes biases, darks, internal and external flat fields at different wavelengths, calibrated sources for measuring instrument throughput, and unresolved sources to monitor imaging quality. These data allow us to measure and track the stability and repeatability of fundamental parameters of the UVIS-1' flight detector and the WFC3 instrument, such as bias level, dark current, read noise, dead and hot/cold pixels, optical throughput, and PSF stability.

The UVIS science monitor was executed a total of ten times during TV3, using WFC3 ground test Science Mission Specifications (SMSs) UV28S01 and UV28S04. Two of these cycles were performed with WFC3 in ambient conditions, during which the UVIS-1' detector was at a temperature of -50° C. The remaining eight cycles were performed under vacuum, with the detector at its expected flight temperature of -82° C. Table 1 lists specific information for each of the ten runs, including dates, the SMS version, which Main Electronics Box (MEB) was

in use, and the section of the overall TV3 test in which the run occurred. For this last item, the abbreviations are as follows: AC-1 = Ambient Calibration 1, SFT = System Functional Test, SC-1 = Science Calibration 1, SC-2 = Science Calibration 2, AC-2 = Ambient Calibration 2.

Table 1. Test Run Information.

Run	Date (UT)	Day	SMS	MEB	CCD Temp	Env	TV3 Section
1	23-Feb-2008	054	UV28S01F	1	-50°	Amb	AC-1
2	06-Mar-2008	066	UV28S01G	2	-82°	T/V	SFT
3	07-Mar-2008	067	UV28S01H	1	-82°	T/V	SFT
4	19-Mar-2008	079	UV28S01H	1	-83°	T/V	SC-1
5	22-Mar-2008	082	UV28S01H	2	-83°	T/V	SFT
6	23-Mar-2008	083	UV28S01H	1	-81°	T/V	SFT
7	29-Mar-2008	089	UV28S01H	1	-82°	T/V	SC-2
8	06-Apr-2008	097	UV28S01H	2	-82°	T/V	SC-2
9	13-Apr-2008	104	UV28S01H	2	-82°	T/V	SC-2
10	21-Apr-2008	112	UV28S04	2	-50°	Amb	AC-2

Test Contents

The UV28S01 SMS consists of a total of 19 exposures. The parameters for the individual exposures are listed in Table 2. All exposures were obtained with the nominal commanded CCD gain setting of 1.5 e^-/DN. The test contains a combination of full-frame and sub-array exposures, as well as unbinned and binned exposures. A combination of internal and external sources were used. Internal flat field exposures were obtained using the built-in WFC3 Calibration Subsystem. External sources were provided by the optical stimulus (OS), which provides individual point and extended sources, as well as flat field illumination. The point-source exposures are used to monitor optical quality and PSF characteristics at two different wavelengths. The extended-source exposures are used in conjunction with stimulus flux measurements of the incident light to monitor the absolute throughput of WFC3 at two wavelengths. Versions F, G, and H of the UV28S01 SMSs listed in Table 1 differed only in exposure times for a few of the exposures, in order optimize signal levels. The UV28S04 SMS is identical to UV28S01H except that the internal D2 flat field exposure was eliminated to satisfy restrictions on the use of the D2 lamp in ambient conditions.

Table 2. UVIS Science Monitor Exposure Parameters.

Exp	Image Type	Time (sec)	Filter	Size	Bin	Amps	Details
1	Bias	0	-	Full	1	ABCD	Full-frame bias
2	Bias	0	-	800x800	1	C	Sub-array bias
3	Dark	300	-	800x800	1	C	Sub-array dark
4	Point	1	F625W	200x200	1	C	HeNe 633nm point source
5	Point	30	F275W	200x200	1	C	Xe 250nm point source
6	Extended	7	F218W	800x800	1	C	Xe 218nm 200μm source with flux calibration
7	Extended	1	F555W	800x800	1	C	Xe 555nm 200μm source with flux calibration
8	Dark	1000	-	Full	1	ABCD	Full-frame dark
9	Int Flat	14	F555W	Full	1	ABCD	Internal Tungsten lamp
10	Int Flat	1.9	F814W	Full	1	ABCD	Internal Tungsten lamp
11	Int Flat	46	F218W	Full	1	ABCD	Internal D2 lamp
12	Ext Flat	705	F225W	Full	3	ABCD	OS Xe lamp
13	Ext Flat	1000	F218W	Full	3	ABCD	OS Xe lamp
14	Ext Flat	140	F555W	Full	1	ABCD	OS Tungsten lamp
15	Ext Flat	62	F814W	Full	1	ABCD	OS Tungsten lamp
16	Dark	300	-	Full	3	ABCD	Binned dark
17	Bias	0	-	Full	3	ABCD	Binned bias
18	Dark	1	-	Full	1	AD	Reverse clocked
19	Dark	1	-	Full	1	BC	Reverse clocked

Data Reduction

The bias, dark, and flat field images included in the science monitor program could in principle be used to calibrate the remaining exposures in the test. However, because much larger bias, dark, and flat field programs were obtained in other tests during TV3, we decided to use the calibration reference files generated from those programs to reduce the science monitor data. Calwf3 version 1.1 was used to process all of the science monitor images, along with bias, dark, and flat field reference files appropriate for the detector temperature and MEB in use for each science monitor run. The calibration reference files were selected from the latest set of files available in CDBS, all of which were generated from TV3 ground-test data.

All exposures were processed with a minimum of the DQICORR (data quality initialization) and BLEVCORR (bias overscan subtration) calibration steps. Processing for biases stopped there. Darks received an additional BIASCORR (bias reference image subtraction) step and flat field images received BIASCORR and DARKCORR (dark reference image subtraction)

processing. Processing of the four external point- and extended-source exposures (exposures 4-7 in Table 2) included all of these steps as well as flat field correction (FLATCORR).

Analysis

Bias Images

Four different types of bias images are included in the science monitor: an unbinned full-frame bias (exposure 1), an unbinned sub-array bias (exposure 2), a 3x3 binned bias (exposure 17), and two unbinned full-frame reverse-clocked biases (exposures 18-19). Even though exposures 18-19 are commanded as a dark, the 1.0 second exposure time and the special CCD readout mode makes them equivalent to a bias. In particular, the readout technique shifts the charge from all the pixels to one of the two amplifiers on each CCD chip, while sampling the output from the other amplifier on the chip. This technique was developed for testing the CCD detector when it is warm, which allows us to measure the read noise of the electronics without being swamped by the high level of dark current at warm temperatures. These exposures were included in the science monitor to allow us to assess its behavior and to correlate its performance against normal bias images.

The calwf3 BLEVCORR step reports the mean bias level measured for each amplifier quadrant during processing. The results for full-frame exposures 1 (unbinned) and 17 (3x3 binning) are shown in Figure 1 and Figure 2, respectively, with the mean and rms scatter for the exposures taken under vacuum (cold detector) listed in Table 3. The sub-array bias exposure (3) did not include any overscan and therefore is not included in these results.

Table 3. Bias levels in full-frame bias exposures.

	Exposure 1		Exposure 17	
Amp	Mean (DN)	σ (DN)	Mean (DN)	σ (DN)
A	2556.5	0.45	2512.4	0.70
B	2543.3	0.28	2498.2	0.78
C	2503.4	1.00	2460.4	0.29
D	2605.6	0.43	2552.7	0.85

Several things are evident from these data. First, the bias levels are systematically different for test runs 1 and 10 in which the detector was warmer. Second, there is no significant difference in the bias levels for exposures taken with MEB 1 and 2. Third, the bias levels for the 3x3 binned mode are systematically different than the unbinned mode. Overall the bias levels in each mode are repeatable to a level of 1 DN or less. Residual signal from image to image after bias level subtraction is ~0.04 DN rms, which indicates that the overall bias level is well tracked and removed by the processing algorithms.

A trend that was noticed in TV1 and confirmed here is the fact that there is a small offset in the bias values measured from the overscan regions of the images relative to the active image

areas. The signal in the image area pixels of unbinned exposures is 0.08-0.11 DN higher than in the overscan regions. In the 3x3 binned images, the offset is ~0.68 DN, approximately 9 times higher, as might be expected. The consequence of this offset is a residual signal in the image areas after the overscan levels have been subtracted. This will not be a problem for calibration, however, because the offset will be present in bias reference images that are subtracted from science images during calibration processing, which will remove the residual signal.

The sub-array bias image (exposure 2) did not include any overscan areas. The mean bias levels measured from the imaging pixels are shown in Figure 3. The relative deviations from one test run to the next is consistent with what was measured for amp C in the full-frame exposures (see Figure 1). The rms scatter in the bias level in the set of 8 TV images is ~0.93 DN, which is also consistent with the scatter in amp C bias levels in the full-frame images (see Table 3).

The readout noise was also measured from the bias images, using the standard deviation of the image area pixel values in each CCD quadrant. The mean noise in the unbinned bias images taken at -82°C is 1.89, 1.98, 1.91, and 1.97 DN (2.9, 3.1, 3.0, and 3.1 e^-) for amps A through D, respectively, and has an rms scatter of ~0.04 DN (0.06 e^-) amongst the 8 runs at that temperature. Noise measured from the reversed-clocked exposures (18 and 19) gives nearly identical results: 1.92, 1.97, 1.87, and 2.00 DN (3.0, 3.1, 3.0, 3.2 e^-) for amps A through D.

Dark Images

Three dark exposures were included in the science monitor: exposures 3, 8, and 16. Exposure 3 is not useful for measuring the dark current because of the short exposure time (300 seconds). The 1000 second exposure time of exposure 8 provides a signal level that is barely adequate for obtaining a dark measurement. Exposure 16 provides an easy measure of the dark because it used 3x3 on-chip binning, which increases the signal per pixel by a factor of 9. The dark current rates measured from exposures 8 and 16 are shown in Figure 4 and Figure 5, respectively. The dark rate in the unbinned TV exposures averages ~0.24 e^-/hour, with a rate of 30-40 e^-/hour when the CCDs were at the warmer temperature of -50°C. These values are in good agreement with results from the dedicated TV3 UVIS dark program (Martel 2008b). Dark rates in the 3x3 binned exposures are fairly stable across all runs, averaging ~7.3 e^-/hour. This is about a factor of 2 higher than what Martel (2008b) reported, although different analysis methods were used and the binned images in the dedicated dark program have much higher signal-to-noise ratios.

PSF Monitoring

Point-source images were obtained at wavelengths of 633 and 250 nm (exposures 4 and 5). The source for the 633 nm exposures was the OS HeNe laser, while the 250 nm measurement used the OS Xe lamp with an 11 nm monochromator bandwidth. Encircled energy (EE) measurements were obtained using the same IDL analysis routines used by Hartig (2008a) to determine the overall WFC3 optical quality and PSF characteristics. Measurements for the sources at 250 nm were obtained within an aperture diameter of 0.20 arcseconds and within a diameter of 0.25 arcseconds for those at 650 nm. Results are shown in Figure 6.

Science monitor test runs 2 and 3 were obtained before the WFC3 optical alignment had been optimized under vacuum and therefore resulted in much lower EE values than the remaining 8 runs. At 250 nm, the mean EE of the 8 good runs is 0.81, with a scatter of only 0.003. At 650 nm, the mean EE is 0.78 with a scatter of 0.006. The mean EE values are in very good agreement with those of Hartig (2008a). The larger scatter in the 650 nm measurements is almost certainly due to the blurring effects of shutter-induced vibrations (see Hartig 2008b). This effect increases the FWHM of sources in exposures with short exposure times (< 5 seconds) and appears to be stronger with one of the two shutter blades. Therefore, in a random set of images such as the 650 nm point-source exposures in the science monitor, some will be blurred more than others depending on the state of the shutter blades for each exposure.

Photometric Monitoring

Exposures 6 and 7 in the science monitor were used to monitor the photometric performance and stability of the WFC3 UVIS channel. These exposures use the OS 200μm source fiber, which results in a source of ~40 pixels in diameter in UVIS images. OS flux calibration measurements were obtained with each of these exposures, which record the source flux incident onto the WFC3 pick-off mirror. Aperture photometry was performed on the calibrated images, with a source aperture diameter of 140 pixels and a sky annulus that extended from 200 to 240 pixels in diameter. The integrated source counts were divided by the OS flux calibration measurements for each image to produce a total WFC3 throughput value.

The results from the ten science monitor runs are shown in Figure 7, where the individual throughput values have been normalized by the mean of the 8 TV runs, showing the relative deviation in throughput from run to run. The rms scatter of the 8 TV runs is 1.5% at 218 nm and 1.0% at 555 nm. If we exclude runs 2 and 3, which were taken while WFC3 was still stabilizing to the vacuum environment and before the optical alignment had been optimized, the rms scatter decreases to 1.0% and 0.6%, which indicates good photometric stability over the course of TV3 testing. There does not appear to be any correlation between throughput and the MEB used (open versus filled symbols in Figure 7).

Flat Field Images

There are a total of seven flat field images included in the UVIS science monitor. Exposures 9-11 were illuminated with the internal Calibration Subsystem and exposures 12-15 used the external OS flat field illumination. Mean flats were formed using the eight exposures taken under thermal-vacuum conditions. Each individual exposure was then divided by the mean flat to assess the quality of the flat fielding and to gauge the stability of the flat field structure over time.

This process revealed an anomaly in the exposures taken during test runs 2 and 6. These exposures are affected by what has been determined to be a Quantum Efficiency (QE) hysteresis problem in the CCDs, such that the QE is several percent lower than normal when the detectors are first turned on after being cooled down. Subsequent full-field illumination of the chips with a total signal equivalent to several times full-well restores the QE to its normal level. Test runs 2

and 6 did in fact occur within hours of the CCDs being recooled and before any other large-scale illumination had occurred. This effect was first noticed during TV1 testing in 2004 (Baggett & Richardson 2004; see also Bushouse & Lupie 2005) and will be discussed in detail in a future ISR. Figure 8 shows the ratio of the F555W internal flat (exposure 9) from test run 2 to the mean F555W flat and illustrates the particular form of the anomaly known as the "elf hat". Similarly, Figure 9 shows the ratio of the F555W internal flat from test run 6 to the mean F555W flat and illustrates the form of the anomaly known as the "bowtie". Due to the presence of this anomaly, the exposures from test runs 2 and 6 were not used in the construction of the mean flats, leaving a total of 6 TV exposures contributing to each mean flat.

The individual exposures for the F555W, F814W, and F218W internal flats (exposures 9-11) and for the F555W and F814W external flats (exposures 14 and 15) had signal levels of ~40,000 e^-. The external F225W and F218W flats (exposures 12 and 13) had signal levels of ~10,000 e^- and 2,000 e^-, respectively. For purely Poisson noise these signal levels should result in flat field accuracies of ~0.5%, 1%, and 2%, respectively. Analysis of the ratios of the individual flat field exposures to the mean flats in fact shows these levels of residual noise. The F225W external flat (exposure 12) is a good example. Figure 10 shows the individual F225W external flat field exposure from test run 8, where the intrinsic flat field structures have peak-to-peak deviations of 10-15%. Figure 11, however, shows the result of dividing that individual exposure by the mean F225W flat and illustrates how the intrinsic flat field structure is completely removed. The rms noise level in the flat-fielded image is ~1%, which is exactly what would be expected from Poisson noise for an exposure with signal of ~10,000 e^-. Results of the same process for the flat field exposures with signal levels of ~40,000 e^- have rms residuals of 0.45-0.5%, which is again just what would be expected for purely Poisson noise. It also indicates that the intrinsic flat field structure is stable to at least 0.5% over the course of the tests, which in this case has a maximum baseline of 38 days.

We have also examined the stability of the internal calibration subsystem lamps by simply tracking the mean signal level in the three internal flats over the 8 TV runs of the science monitor. The results are shown in Figure 12, which shows the mean signal level in each of internal F555W, F814W, and F218W flats (exposures 9-11) relative to the mean of the 8 TV test runs. The Tungsten lamp #1, which was used for the F555W and F814W flats, shows no long-term trend and has an rms scatter over the 8 runs of ~1%. The D2 lamp, however, which was used for the F218W flats, shows an overall degradation in flux of ~10% between test runs 2 and 9. The largest drops occurred between runs 3 and 4, and between 6 and 8, which correspond to the times when the lamp had the greatest use in other TV3 test procedures. This confirms the behavior reported by Baggett (2008).

CEI Verifications

The wide variety of data in the science monitor and the long time baseline over which they were acquired makes this dataset suitable for verifying whether WFC3 meets many of its Contract End Item (CEI) specifications. The following sections address CEI specifications one at a time.

CCD Detector Readout Noise

CEI specification 4.6.3 requires the CCD read noise to be <4.0 e^-/pix rms, with a goal of 3 e^-/pix rms. Analysis of the science monitor bias images has shown read noise to be <3.1 e^-/pix rms in all amplifier quadrants of unbinned images, which meets the requirement and is very close to achieving the goal. This was previously verified by Martel (2008a) through analysis of TV3 dedicated bias programs.

CCD Detector Dark Current

CEI specification 4.6.4 requires the CCD dark current to be <20 e^-/pix/hour. We have shown that dark images from the science monitor have dark current rates of <1 e^-/pix/hour, which easily meet the requirement.

CCD Detector Correlated Noise

CEI specification 4.6.6 requires the level of any correlated noise in the CCD readouts to be limited to <20% of the total rms read noise. The FFT procedures used for WFC3 Electromagnetic Interference (EMI) tests were used to analyze many of the individual bias frames from the science monitor and the results show no correlated noise above a level of ~0.01%, which far exceeds the requirement.

CCD Detector QE Stability

CEI specification 4.6.10 paragraph 1 requires the QE of the CCDs to be stable to better than ±0.5% peak-to-peak over an hour and paragraph 2 requires stability better than ±1.0% peak-to-peak over one month. To check for changes in the overall CCD sensitivity we compared the chip 2 to chip 1 ratios of several F555W external flat field exposures. This procedure essentially uses each chip as a reference for the other in order to remove any effects due to uncontrollable changes in the incoming illumination level and thereby provide a stable comparison from one test run to another. Sigma-clipped means of these ratios show peak-to-peak variations of 0.07% for exposures covering a time span of 31 days, which easily meet the 1% requirement over a month. We do not have exposures taken closely enough in time to directly assess the requirement over a one hour span, but we can safely conclude that if the QE is stable to 0.07% over 31 days then it should surely be stable to <0.5% over one hour.

CCD Detector Flat Field Uniformity

CEI specification 4.6.11.1 paragraph 1 requires that the CCD response shall be correctable to <2% at all wavelengths and to <1% between 400-850 nm, with a goal of <0.5%. The analysis of the science monitor flat field exposures shows residuals in flat-fielded images of 0.45-0.5%. This indicates that we easily meet the requirement and are hovering on the edge of meeting the goal at all wavelengths, which is at the theoretical limit of the noise in the science monitor flats.

Paragraph 2 of this specification (out of range response) requires that <5% of all pixels shall have response outside the range of 90-110% of the mean, with a goal of <1% outside the range

of 95-105%. Analysis of the science monitor flats shows ~0.2% of pixels outside of the 90-110% range and <1% outside of the 95-105% range, which meets the CEI goal.

CCD Detector Flat Field Structure

CEI specification 4.6.11.2 paragraph 1 (low spatial frequency flat field structure) requires that large-scale non-uniformities in the flat field structure shall not exceed 3% peak-to-peak. As was shown earlier, the F218W flats have medium-scale features at a level of ~10% peak-to-peak and the F814W flats also have one medium- to large-scale feature at a level of ~10%, so we do not meet this requirement.

We do, however, easily meet the paragraph 2 specification (flat field large scale correctability), which requires that large-scale non-uniformities shall be correctable to <2%. Flat-field corrected images show no residual large-scale structure (variation in the mean across the detector is <<1%) and have pixel-to-pixel rms residuals of <0.5%.

CCD Detector Non-Functional Pixels

CEI specification 4.6.11.3 requires that <1% of pixels may be non-functional, which includes dead pixels, hot pixels (>100x the mean dark current or 0.1 e^-/sec, whichever is larger), and pixels with uncorrected QE outside the range of 50-200% of the mean QE. Super-darks constructed from TV3 exposures have about 30 pixels > 0.1 e^-/sec, which is ~0.0002%. As shown earlier, the mean flats from the science monitor have <1% of pixels outside of the range 90-110%, which is more restrictive than the 50-200% range of the spec. The WFC3 CCDs therefore easily meet this requirement.

CCD Detector Flat Field Stability

CEI specification 4.6.11.4 paragraph 1 requires that the difference between two flats taken over 60 days shall not exceed 1% rms, with a goal of 0.5%. Ratios of the day 66 to day 104 F814W external flats, which cover a span of 38 days, show rms residuals of 0.7%, which is at the limit of the noise in the images. We expect that this behavior would extrapolate to 60 days, indicating that we meet the requirement. Flats with higher signal would be required to determine whether we meet the goal of 0.5%. The ratios of individual flats to the mean flat constructed from all exposures do in fact reach rms noise levels 0.5% or better.

Paragraph 2 of this specification requires that no more than 5% of pixels shall exceed 5% variation in flats taken over 60 days. Ratios of the day 66 to day 104 F814W external flats, which cover 38 days, again show that <0.1% of pixels have deviations >5%. Most of the pixels with >5% deviation are actually due to slight changes in the vignetting of the OS illumination in the amp B and C corners of the images and are therefore not intrinsic to the CCDs. This requirement is easily satisfied.

CCD Detector Bias

CEI specification 4.6.14 paragraph 1 (bias stability) requires that the bias level over a single CCD row shall be repeatable to <2 e^- rms. Analysis of the raw full-frame bias images in the

science monitor shows that the mean bias signal in a given row has an rms scatter of 0.7 e^- from image to image, which easily meets the requirement.

Paragraph 2 (bias correctability) requires that the bias level for the entire array shall be correctable to <1 e^- rms. Residuals in bias-subtracted bias images from the science monitor are ~0.06 e^- rms, which is well below the requirement.

These requirements were previously verified by Martel (2008a) through analysis of the TV3 dedicated bias programs.

Conclusions

The ten repetitions of the UVIS science monitor that were executed during WFC3 TV3 testing show that the UVIS channel performs well and meets nearly all of its performance and stability requirements, despite the sometimes frequent shut-downs and re-starts (and associated detector warm-ups and cool-downs) that occurred during testing. Bias levels are repeatable and correctable to sub-DN levels. Dark current is very low at ~0.25 e-/hour and also stable to ~0.2 e^- /hour. Encircled energy of point sources is repeatable to <1% and photometric stability is also 1% or better. Flat field correctability and stability is at a level of 0.5% or better.

Acknowledgments

Thanks are due to the large groups of STScI and Goddard staff who tirelessly supported the WFC3 TV3 testing.

References

Baggett, S., 2008, WFC3 ISR 2008-21, "WFC3 TV3 Testing: UVIS Channel Calibration Subsystem Performance."

Baggett, S. and Richardson, M., 2004, TV1 Shift Report, August 29-30, 2004. Available upon request.

Bushouse, H. and Lupie, O., 2005, WFC3 ISR 2005-20, "WFC3 Thermal Vacuum Testing: UVIS Science Performance Monitor."

Hartig, G., 2008a, WFC3 ISR 2008-40, "WFC3 UVIS PSF Evaluation in Thermal-Vacuum Test #3."

Hartig, G., 2008b, WFC3 ISR 2008-44, "WFC3 UVIS Shutter Vibration-Induced Image Blur."

Martel, A., 2008a, WFC3 ISR 2008-22, "WFC3 TV3 Testing: UVIS-1′ and IR4 Noise Trends."

Martel, A., 2008b, WFC3 ISR 2008-23, "WFC3 TV3 Testing: UVIS-1′ Dark Frames and Rates."

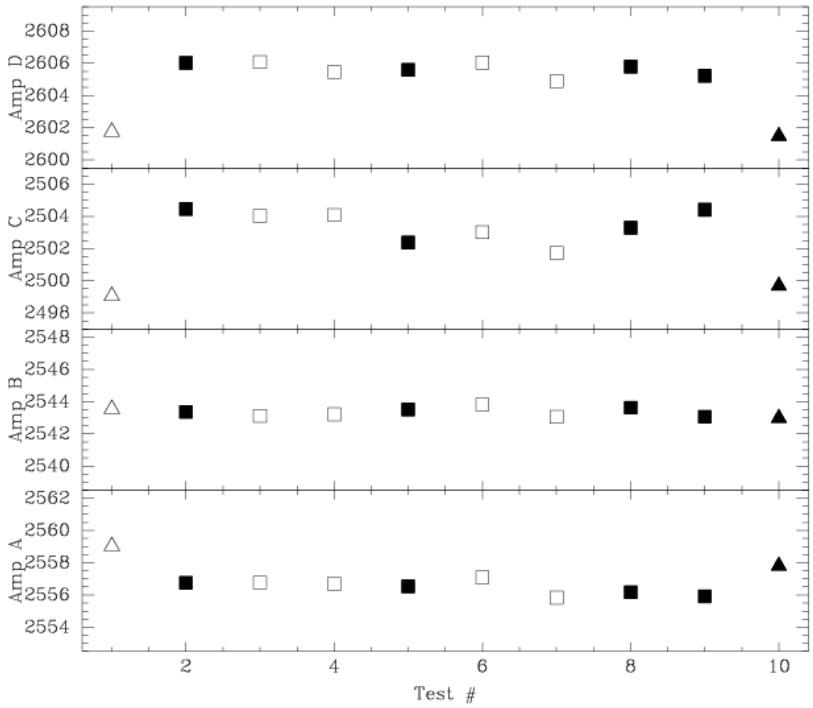

Figure 1. Bias levels for exposure 1 (full-frame, unbinned) in each run of the science monitor. Triangles represent the ambient environment data (wamer CCD temperature) and squares represent the T/V data. Open symbols correspond to MEB 1 and filled symbols MEB 2.

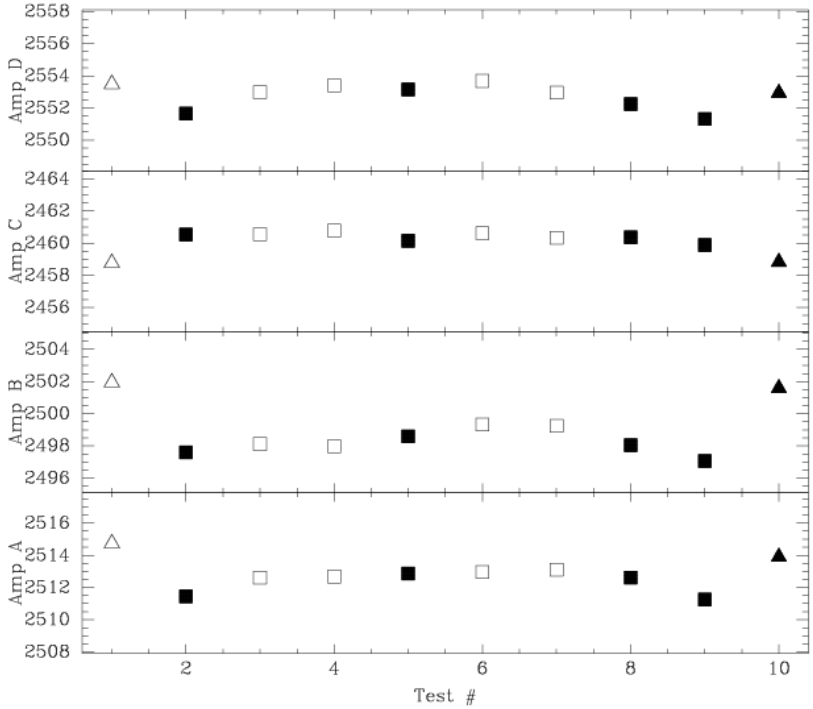

Figure 2. Bias levels for exposure 17 (full-frame, binned 3x3) in each run of the science monitor. Symbols are the same as in Figure 1.

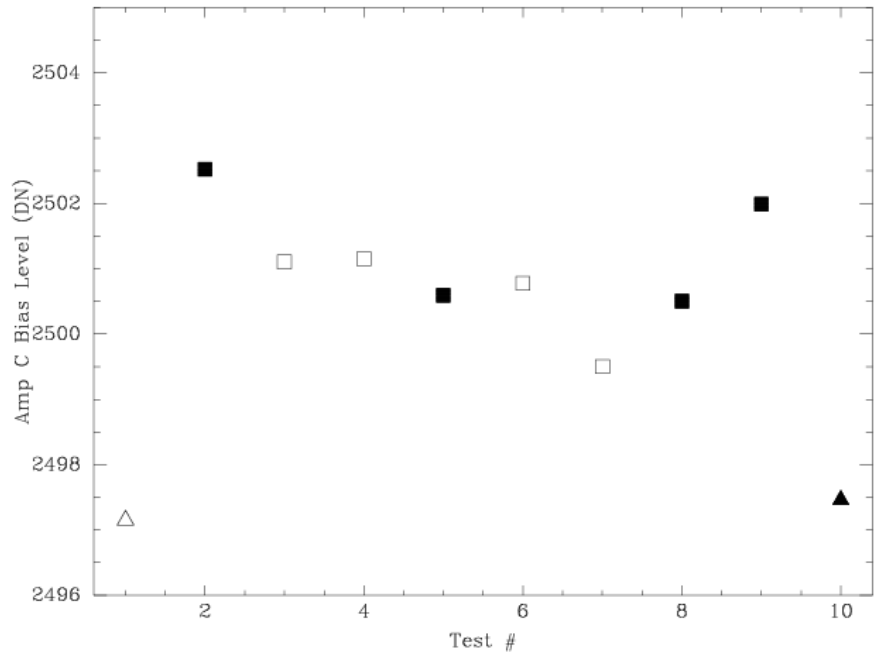

Figure 3. Bias levels for exposure 2 (800x800 sub-array in quad C) in each run of the science monitor. Symbols are the same as in Figure 1.

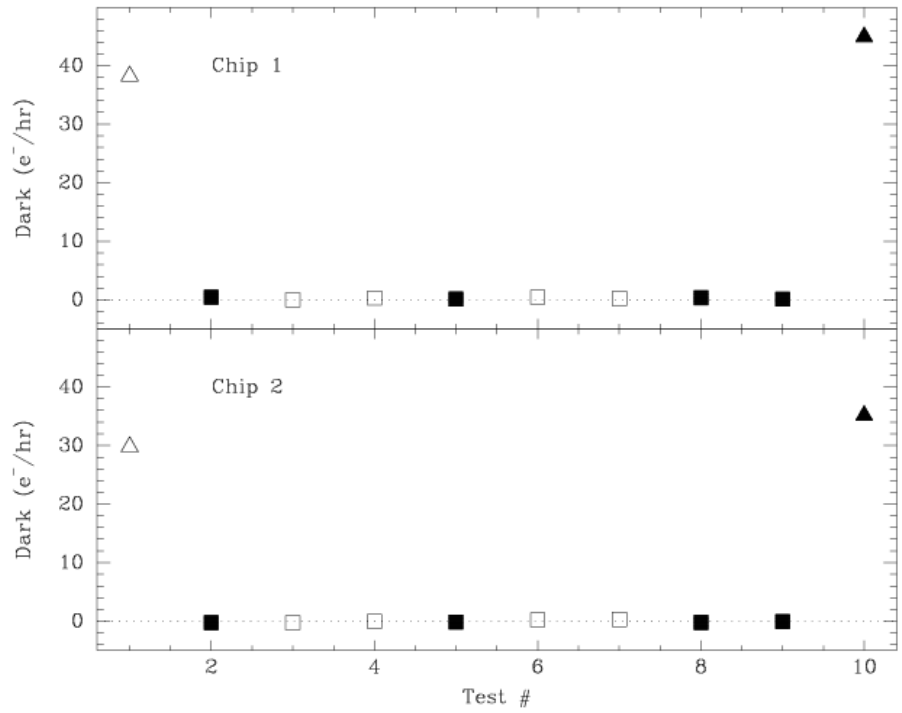

Figure 4. Dark current rates measured from exposure 8 (1000 sec unbinned dark). Symbols are the same as in Figure 1.

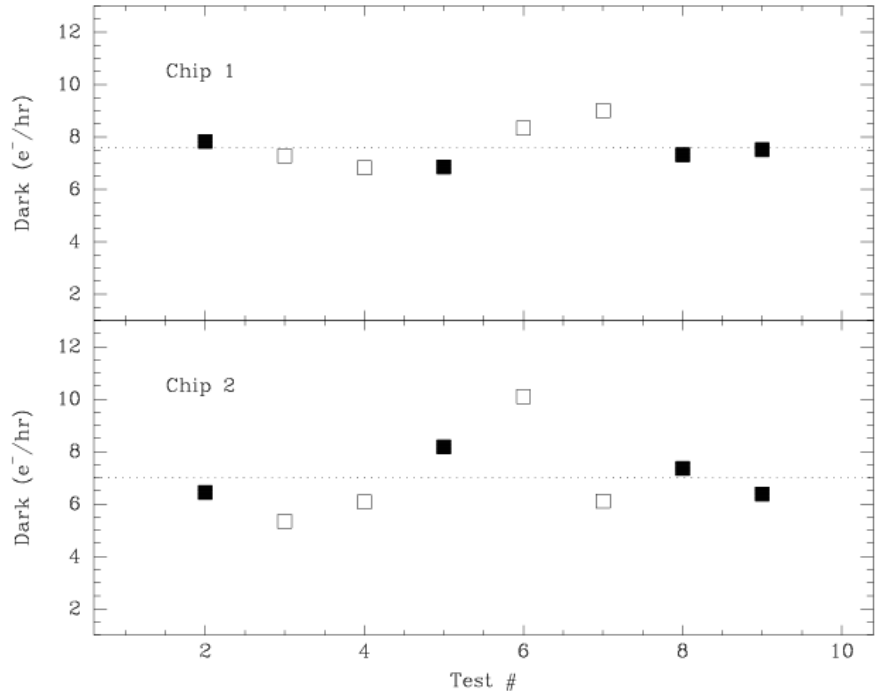

Figure 5. Dark current rates measured from exposure 16 (300 sec 3x3 binned dark). Symbols are the same as in Figure 1. The measurements from the ambient test runs 1 and 10 are not shown because they are so high.

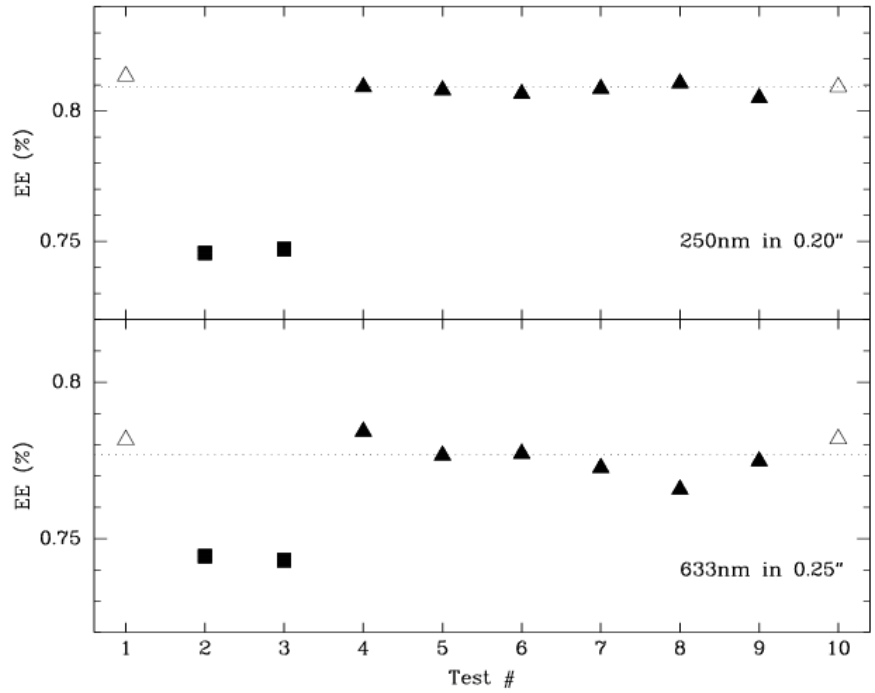

Figure 6. Encircled energy measurements at 250 and 633nm. Test runs 2 and 3 occurred before the WFC3 optical alignment was optimized under vacuum, resulting in lower image quality. The dashed line represents the mean of the remaining 8 runs.

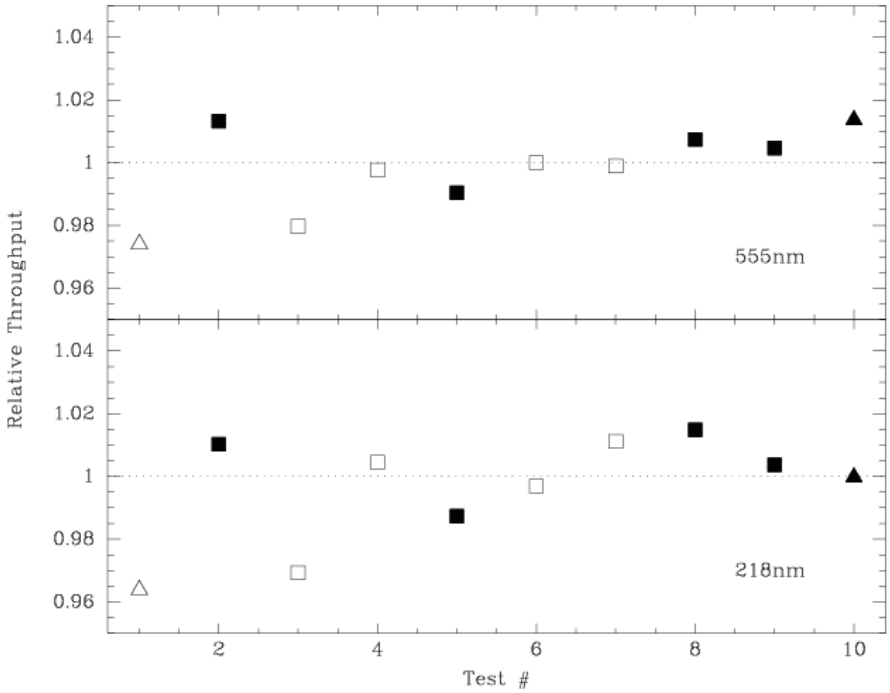

Figure 7. Relative throughput values at 218 and 555 nm from exposures 6 and 7. Symbols are the same as in Figure 1.

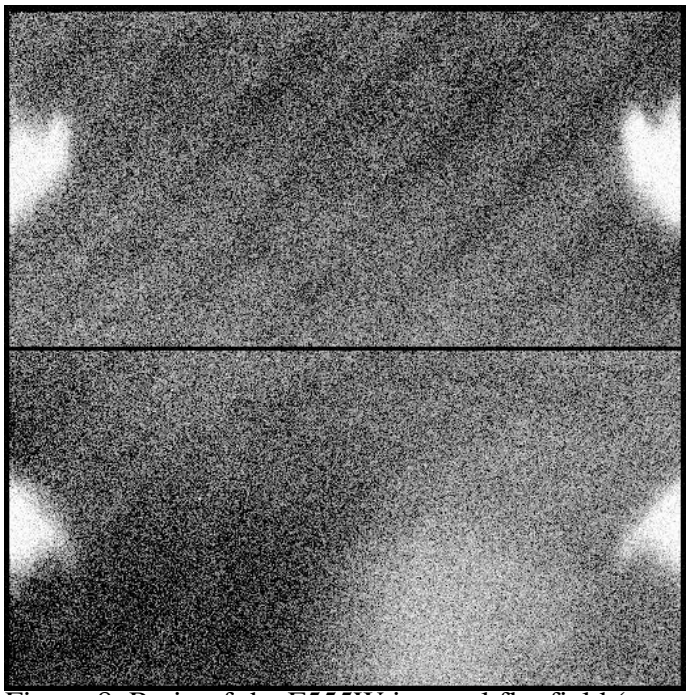

Figure 8. Ratio of the F555W internal flat field (exposure 9) from test run 2 to the mean F555W flat, which shows the turn-on QE anomaly. The bright areas at the left and right edges of each chip have come to be known as the “elf hats”.

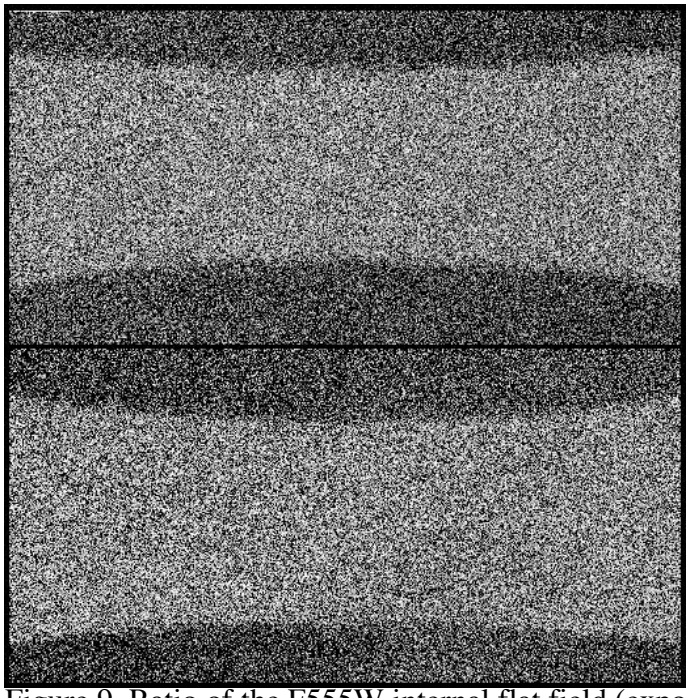

Figure 9. Ratio of the F555W internal flat field (exposure 9) from test run 6 to the mean F555W flat, which shows the turn-on QE anomaly that has come to be known as the “bowtie” due to the shape of the pattern in each chip. The darker areas at the bottom and top of each chip have depressed QE relative to the rest of the chip.

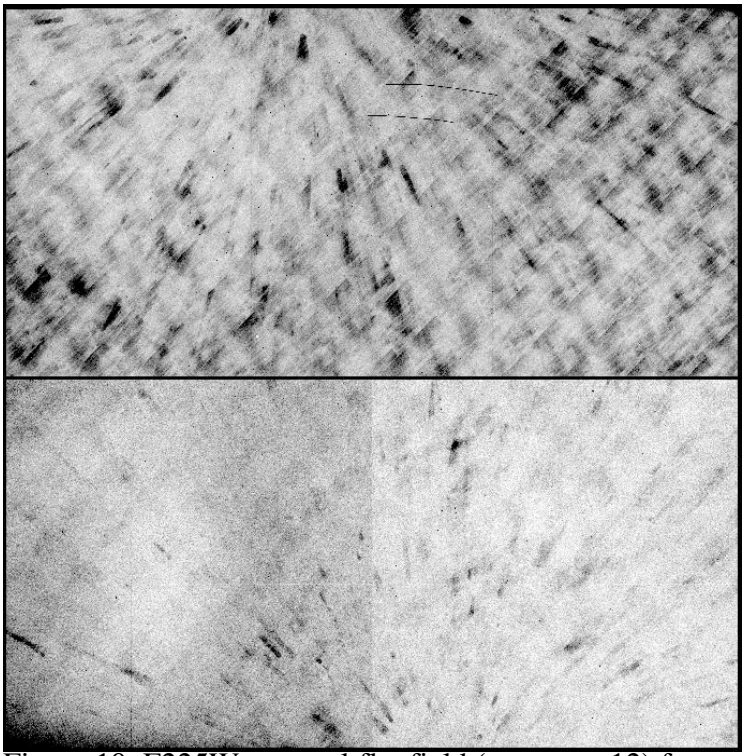

Figure 10. F225W external flat field (exposure 12) from test run 8 displayed with a positive stretch (dark areas are lower signal). The peak-to-peak deviations between the light and dark patches are 10-15%.

Figure 11. The F225W external flat field exposure from test run 8 divided by the mean F225W flat. The residual noise level is ~1.0%.

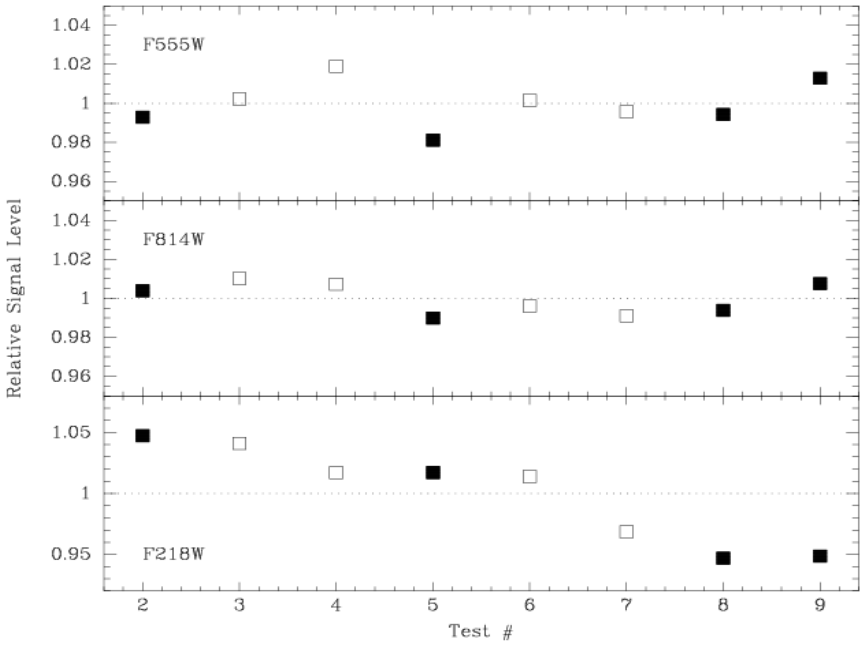

Figure 12. Relative signal levels for the internal flat field exposures 9, 10, and 11 during the 8 TV runs of the science monitor. The rms scatter about the mean for the F555W and F814W flats is ~1%. The D2 lamp, used for the F218W flats, shows an overall decline of ~10% during the test runs.